

DOI: [http://doi.org/10.52716/jprs.v12i1\(Suppl.\).629](http://doi.org/10.52716/jprs.v12i1(Suppl.).629)

## Protection of Oil Refinery Furnaces Bricks Using Coatings of Nano Zirconia-Glass Composites

\*S. A. Zaidan<sup>1</sup>, Hafidh Y. Abed<sup>2</sup>, \*\*Sattar J. Hussein<sup>3</sup>, Hussam J. Mousa<sup>3</sup>, Basim A. Abbood<sup>4</sup><sup>1</sup>Applied Sciences Department, University of Technology, Baghdad, Iraq<sup>2</sup>Ministry of Oil, pipelines company, Baghdad, Iraq<sup>3</sup>Ministry of Oil, Petroleum Research and Development Center (PRDC)<sup>4</sup>Ministry of Oil, Midland Refineries Company –Daura refinery\*Corresponding Author E-mail: [shihab.a.zaidan@uotechnology.edu.iq](mailto:shihab.a.zaidan@uotechnology.edu.iq)\*\*[sattarjaleel@yahoo.com](mailto:sattarjaleel@yahoo.com)6<sup>th</sup> Iraq Oil and Gas Conference, 29-30/11/2021This work is licensed under a [Creative Commons Attribution 4.0 International License](https://creativecommons.org/licenses/by/4.0/).

### **Abstract**

The process of ceramic or refractory surfaces coating is one of the methods used to protect the ceramic body from chemical effects resulting from operating conditions, especially in the applications that include acid gases emissions such as furnaces of petroleum refining units. A mixture of low-melting glass frit was used, reinforced with nano powders of zirconia and Partial Stabilized Zirconia with yttria (3Y-PSZ) with different additives 5wt% and 10 wt%, as well as the addition of nano-alumina for the same percentage of addition. The medium alumina refractory brick which used in lining petroleum refining units was used as a basis for coating.

The coating process was implemented after mixing and preparation of a homogeneous suspension in the presence of water, then drying and sintering until glazing at a temperature of 850 °C. X-ray diffraction technique was used to show the structural characterization of the glazing, which indicated that a glass frit layer was transformed into a mixture of ceramic-glass (crystalline glass), where the crystalline structures of the nano powders were clearly visible. Surface roughness showed low values for frit added with 5wt% of (3Y-PSZ) as well as the frit to which was added 10 %wt of (3Y-PSZ with 5wt% alumina). Moreover, all samples showed clear chemical resistance against acids, including concentrated H<sub>2</sub>SO<sub>4</sub>. Thermal shock resistance varied for vitrification mixtures, but it was good for vitrified samples, adding 10%wt of (3Y-PSZ) with 5wt% alumina as well as adding silicate to the mixture, and these mixtures are considered to be the best in medium alumina refractory surfaces coating.

**Keywords:** Ceramic coating, Glass frit, PSZ, ZrO<sub>2</sub>, Refractory bricks

## حماية طابوق افران المصافي النفطية باستعمال طلاعات من متراكبات زجاج-زركونا النانوية

### الخلاصة

تعتبر عملية طلاء السطوح السيراميكية او الحرارية احد الوسائل المتبعة للمحافظة على الجسم السيراميكي من التأثيرات الكيماوية الناتجة من ظروف التشغيل، خصوصا في تطبيقات تتضمن انبعاث غازات حامضية مثل افران وحدات تكرير المشتقات النفطية. تم استعمال خليط مادة الفرت الزجاجي Glass frit واطئ الانصهار وتدعيمة بمساحيق نانوية من الزركونيا والزركونيا المثبتة جزئياً باليتيريا (3Y-PSZ) بإضافات مختلفة 5wt%, 10 wt% كذلك اضافة الالومينا النانوية لنفس نسبة الاضافة. استعمل الطابوق الحراري متوسط الالومينا المستخدم في تبطين افران وحدات التكرير كأساس يتم طلاءه. بعد اجراء عمليات الخلط وتحضير عالق متجانس بوجود الماء، اجريت عملية الطلاء ومن ثم التجفيف والحرق لغاية التزجيج بدرجة حرارة 850 °C. اجريت الفحوصات التركيبية لطبقة التزجيج باستخدام حيود الاشعة السينية وتبين ان طبقة الفرت الزجاجي تحولت الى خليط من الزجاج السيراميكي (الزجاج المتبلور) وتوضح التراكيب البلورية للمساحيق النانوية بشكل واضح. اما خشونة السطح فقد كانت قيمها منخفضة للفرت المضاف اليه 5wt% من (3Y-PSZ) كذلك الفرت المضاف اليه 10% wt من (3Y-PSZ) مع 5wt% الومينا. كذلك اظهرت جميع العينات مقاومة كيميائية واضحة ضد الحوامض ومنها حاض  $H_2SO_4$  المركز. اما مقاومة الصدمة الحرارية فقد تباينت لخلطات التزجيج ولكنها كانت جيدة للعينات المزججة بالفرت مضاف اليه 10% wt من (3Y-PSZ) مع 5wt% الومينا كذلك باضافة السليكات الى الخليط، وتعتبر هذه الخلطات الافضل في طلاء سطوح الحرارية متوسطة الالومينا.

**الكلمات المفتاحية:** الطلاء السيراميكي، الفرت الزجاجي، الزركونيا المستقرة جزئياً، أكسيد الزركونيوم، الطابوق الناري.

### 1. Introduction

Refractories are widely used in the construction of furnaces for oil refining units. They are either in the form of refractory bricks or refractory mortars. The materials manufactured in refractories are usually characterized by high corrosion resistance. However, these refractories are subjected to chemical reactions resulting from oxidation and reduction conditions or from gases emitted as a result of fuel combustion [1]. Refractory corrosion can be defined as thermal corrosion resulting from a loss in thickness or mass of the refractory material from the surface exposed to heat, as a result of chemical attack by corrosive vapors in a process in which the vapor interacts with the surface of the refractory material. Because of the large difference in the surface energy of the solid thermal phase and gas phase of corrosive vapors, the thermal corrosion process is relatively slow and does not appear in the near range of the start of the operation [2].

Refractories are divided into three types according to the chemical classification (acidic, basic and neutral), so the basic principle of refractory compatibility with corrosive media is the use of acid refractories to resist the acidic environment. Since most of the corrosive fumes and gases emitted from fuel combustion are acidic, such as: (NO<sub>2</sub> and H<sub>2</sub>SO<sub>4</sub>), it requires the use of medium to high refractories alumina and silica in the lining of combustion furnaces. [3]

The acidity or basicity of refractories at high temperatures can be estimated by the ratio of basic to acidic oxides according to the following relationship:

$$V = \frac{\text{Basic Oxide}}{\text{Acid Oxide}} = \frac{\text{CaO} + \text{MgO} + \text{FeO} + \text{MnO} + \dots}{\text{SiO}_2 + \text{P}_2\text{O}_5 + \text{Al}_2\text{O}_3 + \text{Fe}_2\text{O}_3 + \text{Mn}_2\text{O}_3 + \dots} \dots \quad (1)$$

If V is greater than 1, the mixture is basic, and if it is less than 1, it is acidic. [4]

### 1.1 Glazing

Refers to the process of coating the surface with glass materials or chemical oxides. The glaze is a thin and hard layer that covers surfaces and bonds with some of its components. Chemically, it is the transformation of crystallized compounds or oxides into an amorphous (random) structure as a result of rapid melting and cooling of the components. Glazing often aims to:

1. Protection of ceramic parts from pollution and the influence of some acids and alkalis.
2. Giving the surface a smooth texture that prevents the adhesion of impurities.
3. Sometimes it increases the mechanical surface resistance.
4. It closes the pores and prevents the penetration of harmful fumes and gases into the ceramic body [5].

The glaze mixture consists of a group of basic oxides, added to the acid oxides to modify the properties of the glaze from melting (coefficient of thermal expansion, mechanical and physical properties). The most common basic oxides are Na<sub>2</sub>O, K<sub>2</sub>O, Li<sub>2</sub>O, CaO, MgO, BaO) in addition to lead and zinc compounds.

As for the acidic oxides, they are the group of oxides that make up the glass network and are included in the basic composition of the glass, and their ionic potential (ionization energy) is greater than 7 eV. Silica SiO<sub>2</sub> is the most important and widespread acidic oxide. Silica gives the following properties in the composition of glass:

1. It raises the working temperature of the glass and makes it more thermal resistant.

2. It increases viscosity and reduces fluidity.
3. Increase the surface resistance to acids and more mechanical tolerance.
4. It reduces the coefficient of thermal expansion and makes it more compatible with the coefficient of thermal expansion of the ceramic base [6].

Thermal expansion coefficient, glass resistance, flexibility and other factors are parameters that determine the nature of the glazing layer and the following equation can be calculated by which the volumetric thermal expansion coefficient of the glass layer: [7]

$$3\alpha = \beta = w_1\beta_1 + w_2\beta_2 + w_3\beta_3 + \dots w_n\beta_n \dots (2)$$

Where  $\alpha$  is the coefficient of linear thermal expansion ( $K^{-1}$ ),  $\beta$  is the volumetric thermal expansion coefficient ( $K^{-1}$ ),  $w_n$  is the weight fraction of oxides in the glass mixture (wt%) and  $\beta_n$  is the volumetric thermal expansion coefficient of the glass components.

### 1.2 Heat Treatment of the Glaze Layer

The objective of the heat treatment is to incorporate the components of the glaze, and it begins with the evaporation of water and the transformation of silica crystals between (573-226) °C. Thermal treatments also include the volatilization of some basic oxides such as lead and sodium, and some oxides need higher degrees such as calcium and magnesium. The glaze becomes a hard shell when the alkaline oxides, such as sodium and potassium, begin to melt at a temperature of 600 °C, and the reaction continues with the rest of the compounds until the glaze reaches the stage of maturity. [8].

The objective of the project is to prepare a glass mixture dispersed with acid-resistant nanopowders, and coating it on the surfaces of refractories used in lining combustion furnaces, to increase the chemical resistance to corrosion arising from acid gases emitted from the combustion of crude oil.

## 2. Materials and Methods

The refractory bricks whose specifications are shown in Table (1) were cut and used in lining the combustion furnaces of the refining units. Samples were cut to specific dimensions suitable for laboratory testing. Also, the specifications of the materials used in the research and the sources of equipment are shown in Table (2).

**Table (1): Specifications of Burner Refractory bricks.**

Property	units	value
Bulk density	g/cm <sup>3</sup>	2.48
Main chemical components	Al <sub>2</sub> O <sub>3</sub> %	62
	SiO <sub>2</sub> %	32.2
	Fe <sub>2</sub> O <sub>3</sub> %	1.5
	CaO %	1.9
	TiO <sub>2</sub> %	2.4
Cold crushing strength	MPa	52.1
Cold crushing strength after thermal shock at 1200 °C	MPa	49.8
Max. service temperature	°C	1600
Thermal conductivity	W/m.K	(1.05-1.17)
Permanent linear change at 800 °C: at 1200 °C:	%	- 0.12
		- 0.24
Chemical resistance		Acidic resist

**Table (2): Specifications of the materials used.**

Materials	Chemical formula	Grain size	Purity %	Source
Alumina	Al <sub>2</sub> O <sub>3</sub>	80 nm	99.99	Hongwunewmarerial China
Zirconia	ZrO <sub>2</sub>	40-50 nm	99	Hongwunewmarerial China
Stabilized Zirconia	3Y-PSZ	20 nm	99.95	US Research Nanomaterials USA
Lithium hydroxide	LiOH	-----	98.5%	Honeywell, Riedel-de Haën, Germany
Potassium Silicate	K <sub>2</sub> SiO <sub>3</sub>	-----	> 99%	Shanghai Dingkui Biotechnology, China.

Vitreous frit was used whose components are shown in Table (3), and by using a sensitive digital balance (0.01 g), mixtures of frit dispersed with nanopowders were prepared as shown in Table (4). After mixing the mixture and adding 0.75 g of water per 1 g of the vitrification to produce the suspension, one side of the sample surface was coated by a brush with thickness 0.2-0.3 mm. The samples were then dried and fired at 850 °C.

**Table (3): Major oxides for a component of frit.**

Oxides	wt%
SiO <sub>2</sub>	31
Al <sub>2</sub> O <sub>3</sub>	6
PbO	35
Na <sub>2</sub> O	15
CaO	8
Others	5

**Table (4): Components of the prepared mixtures.**

No.	Sample code	Frit wt%	ZrO <sub>2</sub> wt%	3Y-ZrO <sub>2</sub> wt%	Al <sub>2</sub> O <sub>3</sub> wt%	LiOH %wt	K-Silicate %wt
1	F	100					
2	F-5Z	95	5				
3	F-10Z	90	10				
4	F-10Z-5A	85	10		5		
5	F-5YZ	95		5			
6	F-10YZ	90		10			
7	F-10YZ-5A	85		10	5		
8	F-10YZ-10A	80		10	10		
9	F-10YZ-5A-5L	80		10	5	5	
10	F-10YZ-5A-5S	80		10	5		5

### 3. Results and Discussion

#### 3.1. Surface Morphology

The test was carried out by optical microscopy of the surface of the refractory bricks used in the furnaces of refining units. Figure (1) shows the crystalline phases of Mullite (3Al<sub>2</sub>O<sub>3</sub>.2SiO<sub>2</sub>), Cristobalite ( $\alpha$ -SiO<sub>2</sub> resulting from the thermal phase transformation of Quartz crystals) and Corundum ( $\alpha$ -Al<sub>2</sub>O<sub>3</sub> resulted from the thermal phase transition of Gibbsite mineral) and , which are the main components of the alumina medium refractory bricks.[9] Mullite is a crystalline phase with important technical significance because of its excellent technical properties, such as low expansion and thermal conductivity ( $\sim 4.5 \times 10^{-6}$  /°C and 6 W/m.K at 20 °C respectively) and appropriate fracture strength and fracture toughness ( $\sim 200$  MPa and  $\sim 2.5$  MPa m<sup>1/2</sup> respectively).[9]

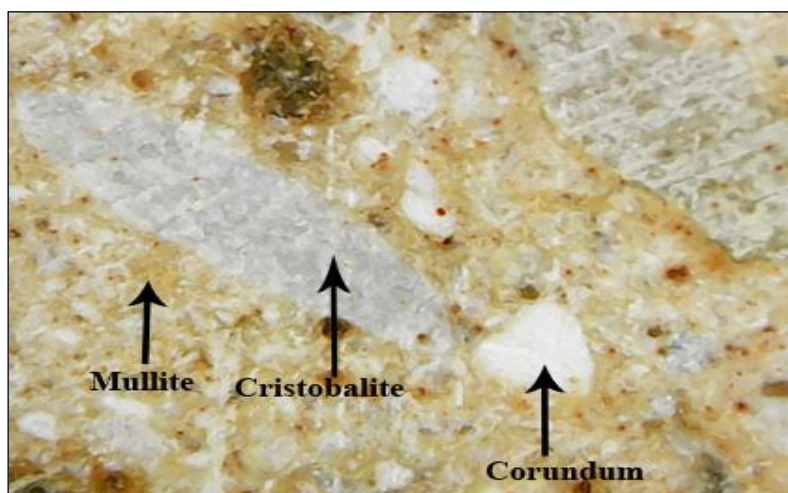


**Fig. (1): Optical microscope image of a refractory brick surface without glaze.**

As for the scanning electron microscopy (SEM) images of the mullite phase region (the most quantified), they showed the shape of the crystal structure of mullite, which is needles-like structures resulting from the transformation of kaolinite sheets into mullite during the firing processes.[10,11] The microstructure of the dominant phase (Mullite) of the refractory brick surface without glazing is shown in Figure 2(a).

After coating the surface of the sample with frit (sample F), the glaze material penetrated between the mullite needles as in Figure 2(b). The surface microstructure of the sample (F-10YZ) in Figure 2(c) shows the distribution of nano partially stabilized zirconia particles between the mullite needles. The glaze acts as a zirconia dispersed matrix of glass – ceramics composite. Increasing the alumina to 10 wt% led to the agglomeration of the nanopowders clearly on the surface of the sample (F-10YZ-10A) and the insufficient temperature of 850°C to melt the mixture as shown in Figure 2(d). The surface structure of the sample (F-5YZ) is shown in Figure 2(e). The image shows a complete melting of frit with its penetration between the mullite needles and the dispersion of nano-zirconia particles. The addition of lithium hydroxide raised the melting temperature of the mixture, and thus the glaze structure was not clear on the surface of the sample (F-YZ-5A-5L) as shown in Figure 2(f).

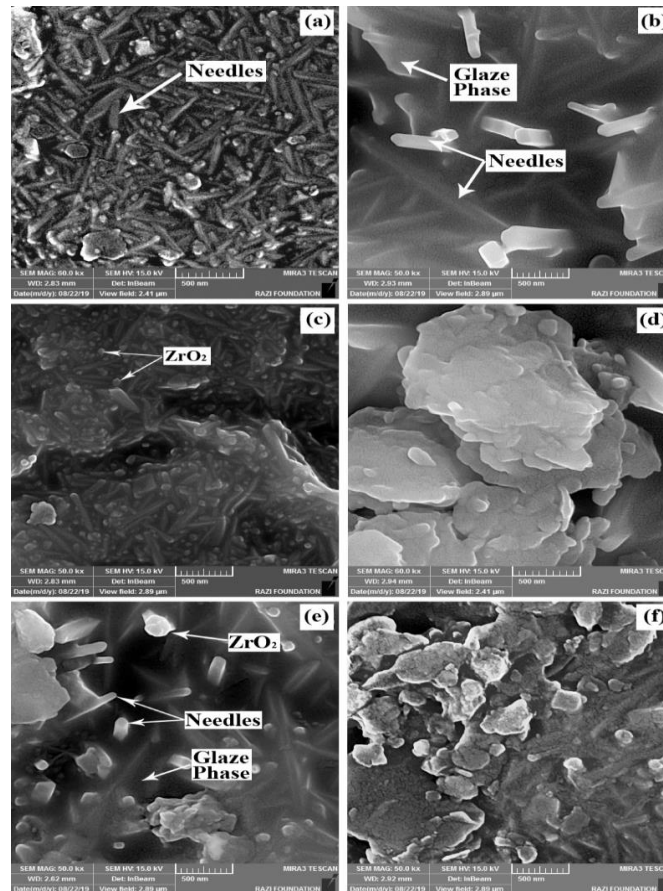


**Fig. (2): SEM image of mullite microstructure.**

Figure (3) (a & b) shows the surface structure of the glazed samples using the optical microscope. It is clear from the sample (F) of the frit-glazed surface only without additions. It is noted that microscopic cracks appeared on the surface because the frit has a high coefficient of thermal expansion compared to the thermal expansion of the refractory substrate [7]. It also shows a complete melting of the frit components at a temperature of 850°C.

While the sample (F-5Z) shows a change in the transparency of the surface by adding 5wt% of  $ZrO_2$ , and this means that the nano-zirconia didn't dissolve chemically in the frit components. However, the glass melted completely with the disappearance of microscopic cracks, and this indicates a decrease in the thermal expansion coefficient of the glass mixture.

According to the relationship (2), increasing the percentage of zirconia to 10wt%, as in the sample (F-10Z), led to a decrease in transparency due to the increase in zirconia and the complete disappearance of microscopic cracks with very smooth of surface. In addition, the glass melting process has been completed. The addition of 5wt% of  $Al_2O_3$ , led to the



appearance of some inhomogeneous spots on the surface, as in the sample (F-10Z-5A), which are areas that are not completely molten due to changing the solubility of the three compounds. While adding 5wt% of Ytria-Stabilized Zirconia as in the sample (F-5YZ), the glaze was homogeneous and did not show obvious microscopic defects. As well as increasing the proportion of yttria-stabilized zirconia to 10wt% for the sample (F-10YZ), the glaze became more homogeneous and completely free of microscopic defects. Moreover, the addition of 5wt%-alumina to the yttria-stabilized zirconia led to a clear improvement in the surface structure without the appearance of any defects as in the sample (F-10YZ-5A). While increasing the percentage of alumina to 10wt%, the images showed a clear heterogeneity in the surface structure and an increase in the amount of blisters on the surface in addition to the lack of complete melting of the glaze layer as shown in the sample (F-10YZ-10A). The addition of lithium hydroxide led to incomplete melting of the glaze mixture, and it needs high temperatures (more than 850 °C) as in the sample (F-10YZ-5A-5L). Finally, 5wt% of potassium silicate was added to the glaze mixture consisting of frit dispersed with 10wt% Ytria-Stabilized Zirconia and 5wt% of  $\text{Al}_2\text{O}_3$ . The pictures showed more melting in the glaze layer and no cracking was observed on the surface as in the sample (F-10YZ-5A-5S).

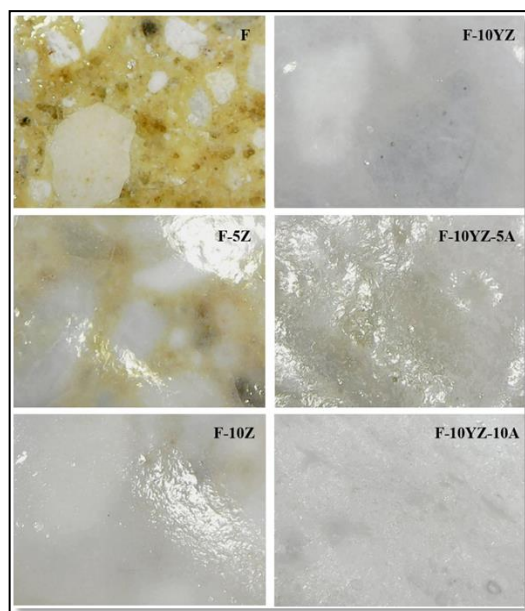


**Fig. (3-a):** Optical microscope images of the surface of the vitrified samples.

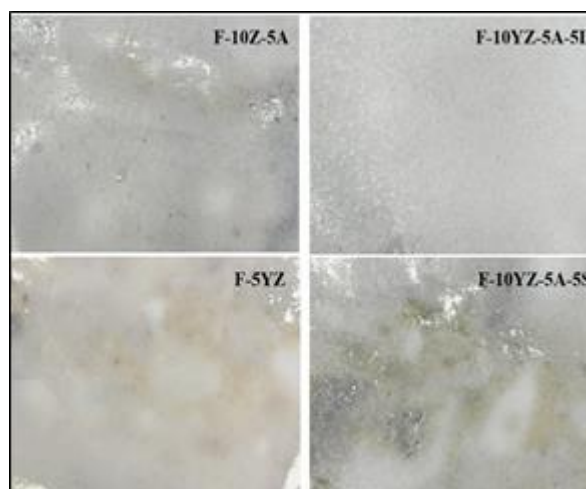


**Fig. (3-b): Optical microscope images of the surface of the vitrified samples.**

### 3.2 XRD Analysis

Figure (4) shows the X-ray diffraction patterns of all layers of the glazed samples. The results of the sample analysis (F) showed that the glaze layer is amorphous structure, and this is a general characteristic for all types of frits. Although the frit oxide components are crystalline structures, the melting of oxides at high temperatures and then rapid cooling led to formation of the amorphous structure. [12] But when adding 5wt% zirconia, as in the sample (F-5Z), it led to the emergence of the crystalline zirconia (monoclinic zirconia  $m\text{-ZrO}_2$  and tetragonal zirconia  $t\text{-ZrO}_2$ ) phases, and this means the change of the glaze layer from Amorphous (glass) state to Amorphous-Crystalline, and then it is called the Glass-Ceramic coating layer.[13] Increasing the amount of zirconia added to 10wt% led to an increase in the percentage of crystal structures, and this is noted from the increase of peaks in the sample pattern (F-10Z). When adding alumina by 5 wt%, multiple crystal structures appeared with zirconia and alumina, in addition to a percentage of amorphous structures (glass) that interfered with the diffraction pattern as in the sample (F-10Z-5A).

The addition of Partially Stabilized Zirconia by Ytria (3Y-PSZ) at a percentage of 5wt% to the glass mixture led to the appearance of peaks of the zirconia (Tetragonal) phase with a large percentage of the amorphous composition of the frit as shown in the sample (F-5YZ). While increasing the amount of partially fixed zirconia to 10wt% led to the emergence of the crystalline phases more clearly and overshadowing the amorphousness of the glass and this is clear from the sample (F-10YZ). As for the addition of 5wt% alumina to the glass mixture

consisting of 3Y-PSZ, it led to an increase in the crystallization of the glass layer, the emergence of crystalline structures, and a clear decline in the amorphousness of frit, as in the sample (F-10YZ-5A). Increasing alumina to 10wt% led to more emergence of zirconia (Tetragonal) phase with alumina as in the sample (F-10YZ-10A). Addition of lithium hydroxide at a percentage of 5wt% led to the emergence of a phase ( $t\text{-ZrO}_2$ ). This means that lithium oxide (after hydroxide is thermally converted to oxide) reduces the percentage of amorphous structures, thus obtaining highly crystallized glaze layer called glass-ceramics. This is shown in sample (F-10YZ-5A-5L). As for the replacement of lithium hydroxide with potassium silicate, this also led to the emergence of the crystal phases and the transformation of the glass layer to ceramic-glass, and this is clear from the sample (F-10YZ-5A-5S).

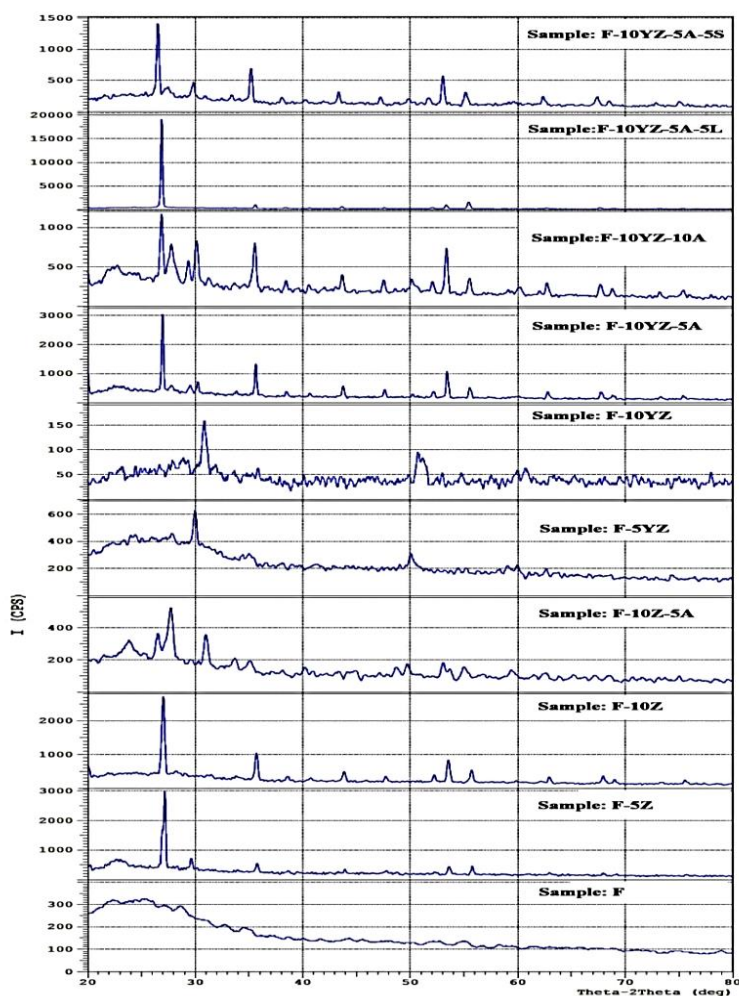


Fig. (4): XRD patterns of surface of glazed samples (M:  $m\text{-ZrO}_2$ , T:  $t\text{-ZrO}_2$  and A:  $\alpha\text{-Al}_2\text{O}_3$ ).

### 3.3 Roughness

This test was performed by the device (TIME3200 Surface Roughness Tester). Figure (5) shows the results of the roughness of the glaze layers. We note that the lowest value of the roughness was (0.374  $\mu\text{m}$ ) for the model (F-5YZ), which means that the vitrification process occurs without the blisters on the surface and a homogeneous distribution of the glass molten on the sample. In comparison with the frit- glazed sample, we notice that the roughness values are close, as shown in the sample (F). generally, the roughness was less than (1  $\mu\text{m}$ ) for the glazed samples by adding 5% wt of zirconia, but it increased by adding alumina as in the sample (F-10YZ-10A). The reason for this is due to the agglomeration of the added nanopowders and their lack of solubility in the frit molten, or due to the compounds resulting from combustion and thus the possibility of damage to the glaze layer.[14] The roughness increased for the structures in which crystallization or granular growth or agglomeration occurs for the added powders, this was evident in the (F-10YZ) and (F-10YS-5A-5L) form of lithium hydroxide and became (2.466  $\mu\text{m}$ ). Although the glass layer was changed to a mixture of (glass-ceramic), the crystal grains led to an increase in the roughness on the surface of the glass layer.

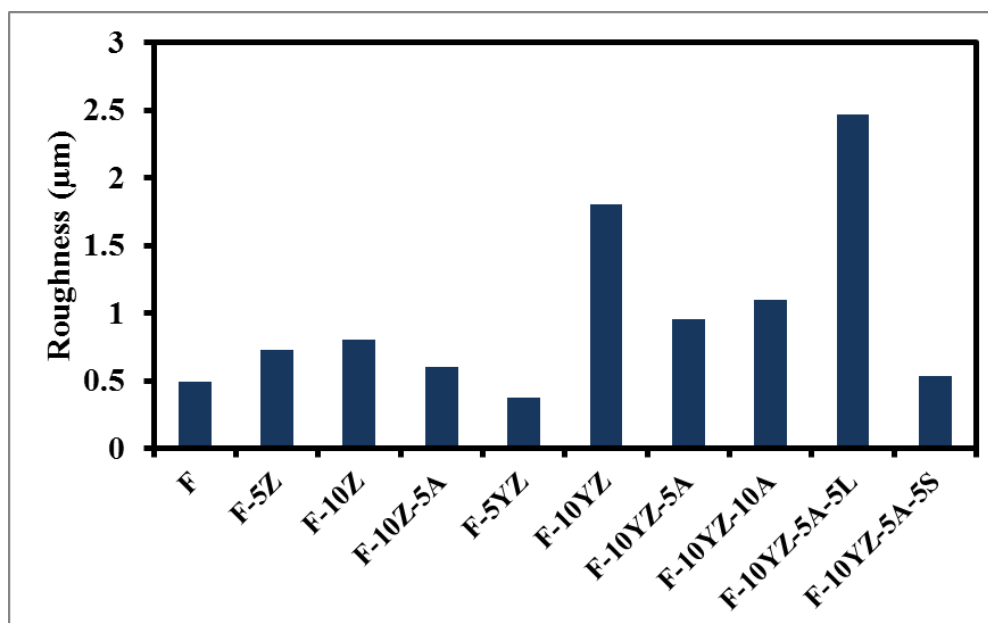


Fig. (5): The roughness of the glaze layers.

### 3.4 Chemical Resistance

The chemical resistance of the glaze layers was achieved according to ASTM C556. It was noted that all the glazed samples showed chemical resistance to the acids, and no change in the surface structure of the glaze layer appeared. The chemical resistance is attributed to the effect of silicon dioxide  $\text{SiO}_2$  (pH=2) and zirconia added  $\text{ZrO}_2$  (pH=4). [15] Therefore, increasing the amount of zirconia will increase the chemical resistance of the frit, especially towards acidic solutions and vapors.

### 3.5 Thermal Shock Resistance

There are two important factors that affect the thermal shock resistance: the coefficient of thermal expansion and the coefficient of thermal conductivity [16] The compatibility between the thermal expansion coefficient of the glaze layer and the ceramic substrate is very important to prevent any cracks due to rapid thermal changes. It is necessary to control the components of the glass transition layer and add materials that have high thermal expansion coefficients such as partially stabilized zirconia by yttria (3Y-PSY) that leads to compatibility with frit.[17] On the other hand, the addition of alumina reduced the coefficient of thermal expansion of the frit to make it compatible with mullite refractories, where its coefficient of thermal expansion is less than  $4.5 \times 10^{-6} \text{ }^\circ\text{C}^{-1}$ . [18] Figure (6) shows micrographs of the surface of the glaze after thermal shock up to  $500 \text{ }^\circ\text{C}$ . Cracks appeared in the glaze layer of samples subjected to thermal shock: F-10Z-5A, F-10YZ-10A, F-5Z, F, F-5YZ, F-10YZ-5A-5L.

The shape of the cracks can be explained on the basis of the difference in thermal expansion coefficients between the components of the glass transition mixture, and the cracks are small and spread on the surface. As for the large cracks, they are due to the difference in the thermal expansion coefficient between the glaze layer and the substrate of refractory brick.

It was found that the sample (A-10YZ-5A) withstood the thermal shock without cracks as well as the sample (F-10YZ-5A-5S), and these samples achieved compatibility between the components of the glass mixture on the one hand and between the layer of glass and the substrate on the other hand.

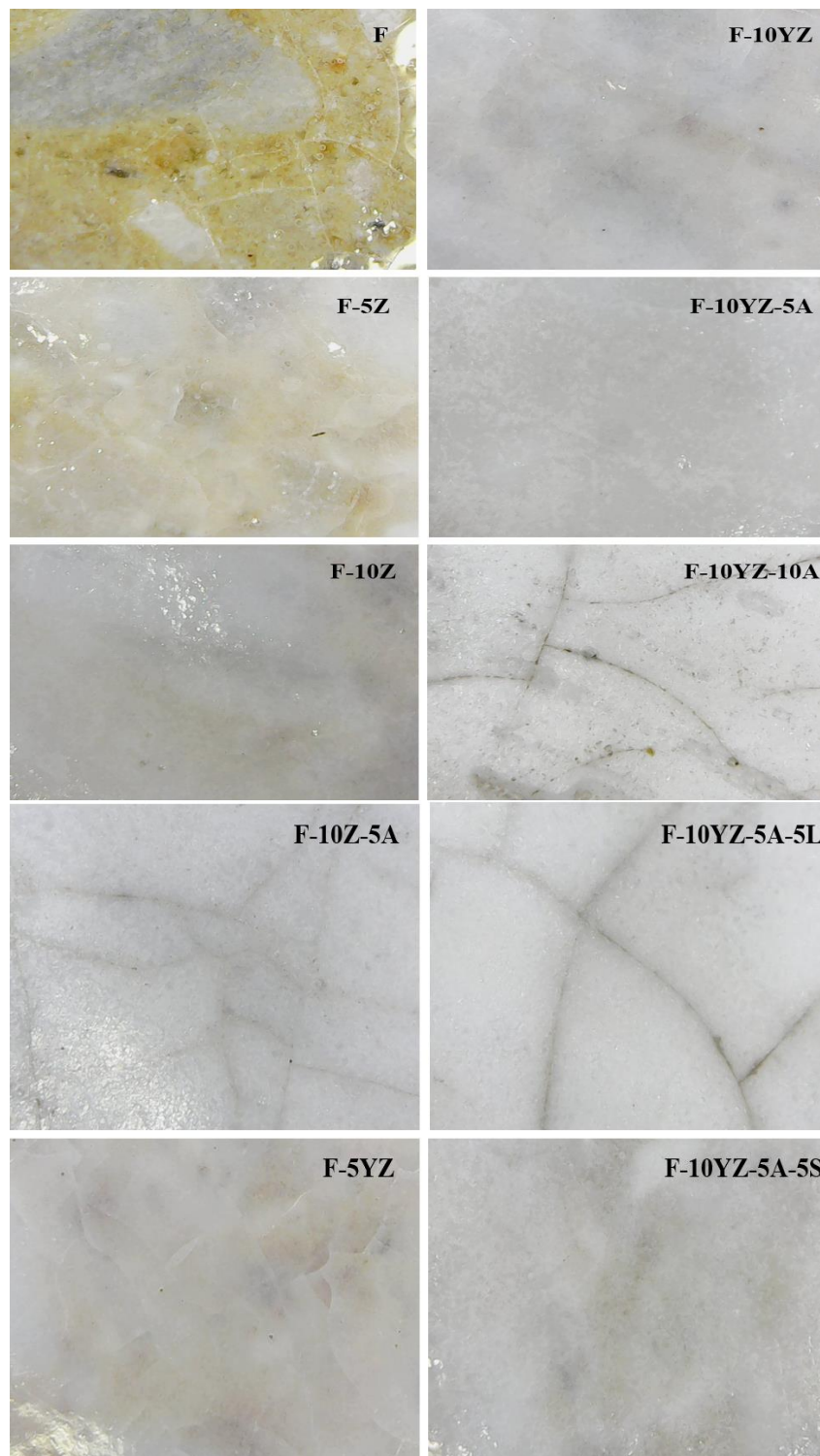


**Fig. (6):** Surface morphology of samples after thermal shock.

#### **4. Application of Nano-coating on bricks for refinery furnaces**

The results of the tests proved the success of the mixtures in obtaining glazed Nano-coating with good specifications such as thermal shock resistance and chemical resistance. One of the mixtures, which is mixture (F-10YZ-5A-5S), was selected for the purpose of applying it on the furnaces of the oil refinery units. The box furnace was selected for the Gasoline Reforming Unit/1 in the Daura refinery as shown in Figure 7(a). After preparing the glaze mixture, a specific area was identified inside the furnace and thoroughly cleaned of dust (Figure 7(c)). The surface of the refractory bricks is coated with a layer of glaze using a brush (Figure 7(b)), with a thickness ranging between 0.2-0.3 mm. The coating layer shown in Figure 7(d) is left to dry and is heat treated by oven heat during operation.

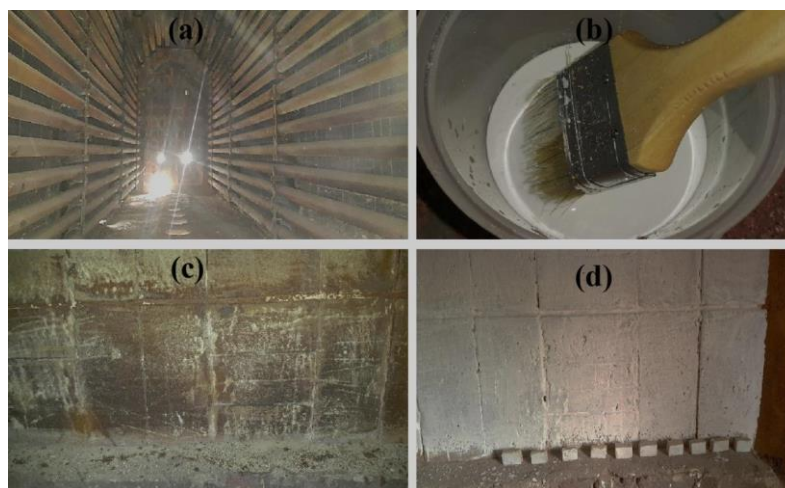


**Fig. (7): Application of nano glaze coating, (a) box furnace for the Gasoline reforming Unit/2 in the Daura refinery, (b) Glazing mixture and paint brush, (c) Furnace wall after cleaning, (d) Furnace wall after coating.**

## **5. Conclusions**

- 1- The addition of Nano- Partially Stabilized Zirconia with Yttria (3Y-PSZ), achieved good results in terms of low surface roughness. Also, adding 5 wt% nano-alumina to the mixture contributed to improving the thermal endurance properties.
- 2- The addition of Potassium Silicate improved the adhesion of the glass layer during the coating process and also contributed to improving the smoothness of the surface.
- 3- The possibility of using mixtures in coating the surfaces of high alumina refractories with thermal tolerances greater than 500°C.
- 4- Increasing the heat treatment temperature of the glaze layer and the operating time leads to an increase in the amount of crystallized phases.
- 5- The glass coating dispersed with nano-ceramic powders becomes a glass-ceramic coating, thus greatly improving the surface properties and thermal resistance compared to the frit-glass coating only.
- 6- Glass coatings prepared from the addition of lithium hydroxide can be used in coating refractories used at temperatures higher than 850°C.



## References

- [1] Cardarelli, F., 2008. Ceramics, refractories, and glasses. *Materials handbook: a concise desktop reference*, pp.593-689.
- [2] Mahapatra, M.K., 2020. Review of corrosion of refractory in gaseous environment. *International Journal of Applied Ceramic Technology*, 17(2), pp.606-615.
- [3] Sengupta, P., 2020. *Refractories for the Chemical Industries*. Springer International Publishing AG.
- [4] Schacht, C. ed., 2004. *Refractories handbook* (Vol. 178). CRC Press.
- [5] Casasola, R., Rincón, J.M. and Romero, M., 2012. Glass–ceramic glazes for ceramic tiles: a review. *Journal of Materials Science*, 47(2), pp.553-582.
- [6] Bou, E., Moreno, A., Escardino, A. and Gozalbo, A., 2007. Microstructural study of opaque glazes obtained from frits of the system: SiO<sub>2</sub>-Al<sub>2</sub>O<sub>3</sub>-B<sub>2</sub>O<sub>3</sub>-(P<sub>2</sub>O<sub>5</sub>)-CaO-K<sub>2</sub>O-TiO<sub>2</sub>. *Journal of the European Ceramic Society*, 27(2-3), pp.1791-1796.
- [7] Plesingerova, B. and Kovalcikova, M., 2003. Influence of the thermal expansion mismatch between body and glaze on the crack density of glazed ceramics. *Ceramics-Silikáty*, 47(3), pp.100-107.
- [8] Hopper, R., 2008. *The Ceramic Spectrum: A Simplified Approach to Glaze & Color Development*, Second Edition. American Ceramic Society Company.
- [9] Romero, M., Padilla, I., Contreras, M. and López-Delgado, A., 2021. Mullite-Based Ceramics from Mining Waste: A Review. *Minerals*, 11(3), p.332.
- [10] Martín-Márquez, J., Rincón, J.M. and Romero, M., 2010. Mullite development on firing in porcelain stoneware bodies. *Journal of the European Ceramic Society*, 30(7), pp.1599-1607.
- [11] Chargui, F., Hamidouche, M., Belhouchet, H., Jorand, Y., Doufnoune, R. and Fantozzi, G., 2018. Mullite fabrication from natural kaolin and aluminium slag. *boletín de la sociedad española de cerámica y vidrio*, 57(4), pp.169-177.
- [12] Li, W., Li, J., Wu, J. and Guo, J., 2003. Study on the phase-separated opaque glaze in ancient China from Qionglai kiln. *Ceramics international*, 29(8), pp.933-937.

- 
- [13] Wan, W., Feng, Y., Yang, J., Bu, W. and Qiu, T., 2016. Microstructure, mechanical and high-temperature dielectric properties of zirconia-reinforced fused silica ceramics. *Ceramics International*, 42(5), pp.6436-6443.
- [14] Sheikhattar, M., Attar, H., Sharafi, S. and Carty, W.M., 2016. Influence of surface crystallinity on the surface roughness of different ceramic glazes. *Materials Characterization*, 118, pp.570-574.
- [15] Sinex, S.A., Halpern, J.B. and Johnson, S.D., 2017. General Chemistry for Engineers in the 21st Century: A Materials Science Approach. *MRS Advances*, 2(31), pp.1629-1634.
- [16] Li, K., Wang, D., Chen, H. and Guo, L., 2014. Normalized evaluation of thermal shock resistance for ceramic materials. *Journal of Advanced Ceramics*, 3(3), pp.250-258.
- [17] Zaidan, S.A., 2017. Improvement the Chemical Resistance of Furnaces Bricks for Petroleum Refineries by ZrO<sub>2</sub>-Nano-Glass-Ceramic Coated. *Engineering and Technology Journal*, 35(10 Part A).
- [18] Cui, K., Zhang, Y., Fu, T., Wang, J. and Zhang, X., 2020. Toughening mechanism of mullite matrix composites: A Review. *Coatings*, 10(7), p.672.